ELSEVIER

Marine and Petroleum Geology 21 (2004) 1073–1081

Marine and Petroleum Geology

www.elsevier.com/locate/marpetgeo

Crustal-scale structure of the South Caspian Basin revealed by deep seismic reflection profiling

Camelia C. Knapp[a,b,c,*], James H. Knapp[a,b], John A. Connor[d]

[a]*Department of Geological Sciences, University of South Carolina, 205 EWS, 701 Sumter St., Columbia, SC 29208, USA*
[b]*Department of Geological Sciences, Cornell University, Ithaca, NY 14853, USA*
[c]*National Institute for Earth Physics, P.O. Box MG-2, Bucharest-Magurele, Romania*
[d]*Chevron Overseas Petroleum Azerbaijan Ltd., 340 Nizami St., 370000 Baku, Azerbaijan*

Received 4 September 2001; received in revised form 5 April 2003; accepted 7 April 2003

Abstract

Two deep seismic reflection profiles from the South Caspian basin provide the first normal-incidence image of possibly the thickest sedimentary basin in the world. Significant features imaged with these seismic data are: (1) a series of high-amplitude folds, developed within a thick (>10 km) Neogene sedimentary section, bounded discordantly below by (2) a gently N-dipping, intermittent reflection at 14–20 km (8.0 + s), (3) a prominent deep reflector at 26–28 km depth (12.8–13.0 s) with a gentle northward dip, (4) an underlying layered interval with discernibly lower-frequency reflections down to ~36–40 km (16.0–16.5 s), and (5) a noticeable decrease in reflectivity below ~36–40 km. Based on the downward termination of fault-cored folds and their discordance with subhorizontal underlying reflections, the reflection at 14–20 km is interpreted to be the basal detachment for structures associated with the Absheron Ridge. The bright reflection at ~26–28 km depth is interpreted as the basement/cover contact, and the underlying ~10 km portion of the section is interpreted as crystalline basement. Downward diminution of reflectivity at ~36–40 km is thought to represent the Moho despite the absence of a clearly reflective horizon. These interpretations are consistent with previous velocity models from both seismic refraction and teleseismic studies in the South Caspian region that suggested a minimum sedimentary thickness of 20 km and a crustal thickness of 35–40 km. Both the apparent lack of local structural relief on the basement reflector, and seismic velocities ($V_p \approx 6.8$ km/s) obtained from earlier studies suggest this crust is not thinned continental material. Although thicker than typical oceanic crust (6–8 km), the apparent ~10 km thickness of the South Caspian crystalline crust is interpreted to be of oceanic affinity for this part of the basin. Active seismicity down to mantle depths (80 km) and gentle deepening of the crust from south to north suggest northward subduction of the South Caspian oceanic lithosphere beneath the continental lithosphere of the Central Caspian basin.

Keywords: South Caspian basin; Reflection profiling; Subduction

1. Introduction

Sedimentary basins have been a dominant aspect of the Earth's crust since the Archean time (McKenzie, Nisbet, & Sclater, 1980), and have long been of interest for their resource potential. Previous studies (Watts, 1992) suggested that the thickest sediments (10–15 km) accumulate at continental margins (Grotzinger & Ingersoll, 1992; McKenzie, 1978), on the continental crust at or near the shelf break in the continental slope (Curray, Emmel, Moore, & Raitt, 1982). In contrast, sediments in excess of 2 km were rarely found to accumulate on oceanic crust, unless the sediments were derived from continental material deposited at continental margins by major river systems such as the Amazon, Niger, Mississippi, Ganges or Colorado Rivers (Watts, 1992). Yet, such basins do not commonly exceed ~15 km thickness in sediment accumulation.

The Caspian Sea basins of Central Eurasia constitute one of the major petroleum provinces of the world (Devlin et al., 1999), and one of the most enigmatic basin systems worldwide. The South Caspian basin evolved adjacent to the rapidly uplifting Greater Caucasus Mountains since the Paleogene (Adamia, Buadze, & Shavishvili, 1977; Zonenshain & Le Pichon, 1986). Several kilometers of

* Corresponding author. Address: Department of Geological Sciences, University of South Carolina, 205 EWS, 701 Sumter St., Columbia, SC 29208, USA.

0264-8172/$ - see front matter © 2004 Elsevier Ltd. All rights reserved.
doi:10.1016/j.marpetgeo.2003.04.002

Plio-Pleistocene clastic sediments that originated in the paleo-Kura, Volga, and Amu Darya rivers (Brunet, Korotaev, Ershov, & Nikishin, 2003) overlay the Mesozoic and Paleogene sedimentary sections (Devlin et al., 1999; Zonenshain, Kuzmin, & Natapov, 1990). An important part of these sediments derived from the eroding Lesser and Greater Caucasus Mountains that formed as the Arabian Plate collided with Eurasia (e.g. Jackson, Priestley, Allen, & Berberian, 2002; Zonenshain et al., 1990).

Situated within the Alpine–Himalayan collisional zone, the Caspian Sea separates the locus of Neogene continental collision in the Caucasus Mountains to the west from large-scale transpressional faulting in the Kopeh-Dagh fold belt to the east (Fig. 1; Jackson, 1992; Jackson et al., 2002). Beneath the Caspian Sea, this boundary is marked by the Absheron Ridge, which represents the division between the Central and South Caspian basins and is the site of major oil fields (Devlin et al., 1999). This change in deformational style across the Caspian Sea from continental subduction in the west to transpressional deformation in the east constitutes a key target for understanding the tectonic evolution of this basin and its present day structure and deformational style.

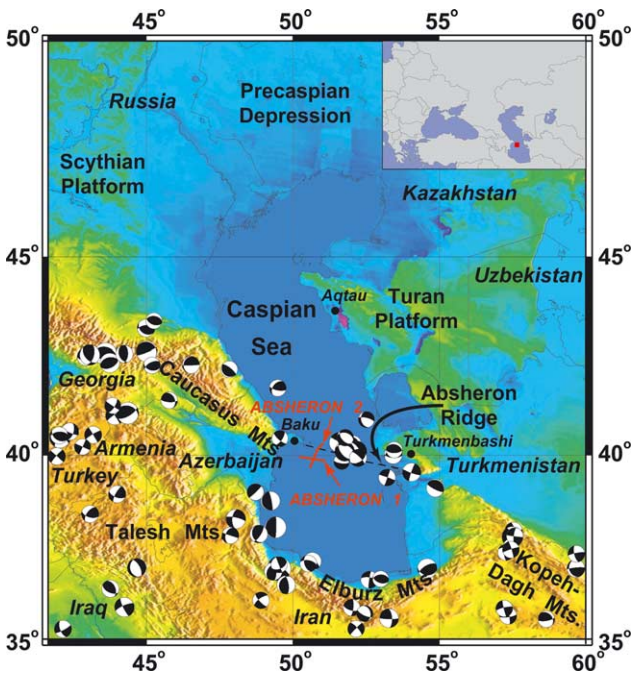

Fig. 1. Location map of the ABSHERON deep seismic reflection profiles on a hillshaded digital elevation model of the Caspian Sea region. Focal mechanisms of earthquakes (Mb > 5.0) within the Caspian Sea and surrounding areas from the CMT catalogue (Harvard, USA) are displayed as beach balls. Abundant seismicity occurs not only in the Caucasus, Elburz, and Kopeh-Dagh Mts., but also along the Absheron Ridge, where the ABSHERON profiles are located. Note the combination of oblique thrust, normal faulting, and strike–slip events along the Absheron Ridge, and the relative absence of seismicity within the central portion of the South Caspian basin. Latitude is shown in degrees east; longitude is shown in degrees north. Inset shows the geographic location of the Caspian Sea within Central Eurasia.

Knowledge of the deep crustal structure of the South Caspian basin has previously been limited to broad seismic velocity patterns provided by Deep Seismic Sounding (DSS) studies (Baranova, Kosminskaya, & Pavlenkova, 1991; Galperin, Kosminskaya, & Kraksina, 1962; Gegelyantz, Galperin, Kosminskaya, & Krafshina, 1958; Zonenshain et al., 1990; Zonenshain & Le Pichon, 1986), without the higher resolution provided by the seismic reflection methods. These early studies suggested that the South Caspian crust is composed of an upper sedimentary layer, with a mean compressional wave velocity (V_P) of 3.5–4.0 km/s, and a lower oceanic ('basaltic') layer with $V_P = 6.6$ km/s (Baranova et al., 1991; Galperin et al., 1962; Gegelyantz et al., 1958). More recent studies on the crustal structure of the South Caspian basin from teleseismic receiver function analysis (Jackson et al., 2002; Mangino & Priestley, 1998) suggested that the Moho [the seismically defined crust–mantle boundary (Jarchow & Thompson, 1989)] beneath the South Caspian basin is an arch-like interface at the depth of ~30 km, making for a much thinner crust than a 45–50 km, north of the Absheron Ridge, beneath the Central Caspian basin. A previous, relatively deep (12 s), seismic reflection profile of the South Caspian basin displays a detailed image of the stratigraphy of the sedimentary section, but unfortunately, for most part did not reach the crystalline basement (Nadirov, Bagirov, Tagiyev, & Lerche, 1997). However, despite the relatively large amount of earlier geophysical investigations of the South Caspian Sea region, the thickness and structural style of deformation of the sedimentary section as well as the crustal thickness and affinity remain equivocal.

The new deep (20 s) seismic reflection data presented here provide evidence that the South Caspian basin may represent one of, if not, the thickest (26–28 + km) accumulation of sediments in the world. These seismic data elucidate the shallow structural deformation, depth, and geometry of the detachment system as well as the definition of the sediment/crystalline boundary, providing new constraints to the previous studies (e.g. Allen, Vincent, Ismail-zadeh, Simmons, & Anderson, 2002; Baranova et al., 1991; Brunet et al., 2003; Jackson et al., 2002), and revealing new information especially at large depths. In addition, these data shed light on the affinity of the crust and the nature of the boundary between the South and Central Caspian basins across the Absheron Ridge which have recently been subject of controversy.

2. Geologic setting

The geology of the Caspian Sea basins has traditionally been divided into four areas (Zonenshain et al., 1990; Zonenshain & Le Pichon, 1986). In the north, the Precaspian Depression is thought to be floored by Devonian oceanic crust (Brunet, Volozh, Antipov, & Lobkovsky, 1999). South of this area, the North and Central Caspian

regions are situated above a Paleozoic basement of the Eurasian craton (Scythian and Turan platforms in Fig. 1; Berberian, 1983; Gegelyantz et al., 1958). South of the Absheron Ridge, the South Caspian basin is believed to be floored by a late Paleozoic–Triassic or late Mesozoic–early Tertiary oceanic crust as inferred from previous geophysical investigations (Amursski, Tiunov, Khrikov, & Shlezinger, 1968; Avdeev, Dubrovski, Fainberg, Pankratov, & Zinger, 1984; Berberian, 1983; Brunet et al., 2003; Jackson et al., 2002; Mangino & Priestley, 1998; Zonenshain et al., 1990; Zonenshain & Le Pichon, 1986).

Previous DSS studies documented a large thickness of the South Caspian sedimentary cover (20–25 km; e.g. Zonenshain et al., 1990). Onshore drilling in Azerbaijan and Turkmenistan, that penetrated part of the sedimentary sequence, found sediments ranging from Late Jurassic to Pleistocene in age which were deposited in shallow water environments (Berberian, 1983; Devlin et al., 1999; Zonenshain et al., 1990). Based on shallow seismic reflection profiling (Zonenshain & Le Pichon, 1986) the youngest of these sediments were traced into the deepest part of the South Caspian basin that reveals large-scale Pliocene–Pleistocene folding and nappe development (e.g. Berberian, 1983; Devlin et al., 1999). Although this basin is thought to have originated in the Mesozoic time, as much as 8–10 km of Plio-Pleistocene sediments have accumulated, representing average depositional rates of ~2.0 km/My for the last 5 million years (Brunet et al., 2003; Nadirov et al., 1997). Abundant seismicity and extensive natural seepage of oil and gas as well as the presence of numerous (over 400) gas-driven mud volcanoes (Bagirov & Lerche, 1999) indicate that the South Caspian basin geologic structures are actively deforming, and abundant hydrocarbons are migrating throughout the basin.

With respect to the origin of the South Caspian basin, earlier studies proposed that it formed as a result of the eclogitization and subsidence of the continental crust during the mid- to late Cenozoic time (e. g. Shlezinger & Yanshin, 1981). Others considered the South Caspian basin to be a remnant of the Early Mesozoic Tethys Ocean (Allen et al., 2002), or a remnant back-arc basin formed behind a Late Cretaceous–Paleogene volcanic arc (Adamia et al., 1977). Shikalibeily and Grigoriants (1980) suggested that the basin is Jurassic in age, and is overlain by Cretaceous age volcanic rocks.

Earthquake seismology studies (Jackson, 1992; Jackson et al., 2002; Mangino & Priestley, 1998; Priestley, Baker, & Jackson, 1994) have suggested that the South Caspian basin is a relatively rigid aseismic block within the active Alpine–Himalayan orogenic belt (Fig. 1). Study of focal mechanisms of historic earthquakes in the South Caspian area and vicinity (Jackson et al., 2002; Priestley et al., 1994) showed that this region is dominated by a compressional regime resulting from convergence between the Arabian and Eurasian plates (Fig. 1). According to Priestley et al. (1994), the convergence between northern Iran and the South Caspian Sea is partitioned into a left-lateral strike–slip and pure thrust motion in the Elburz Mountains, resulting in the northward thrusting of the Iranian continental crust over the South Caspian Basin. The Absheron Ridge region that marks the northern boundary of the South Caspian Sea (Fig. 1) is characterized by normal faulting events parallel to the ridge with depths of 30–50 km (Fig. 1; Jackson et al., 2002; Priestley et al., 1994). Based on the same studies, two deeper (<75 km) thrust earthquakes were localized further to the north-east. Thrust focal mechanisms in the Talesh Mountains, bordering the South Caspian Basin to the southwest (Fig. 1), suggest thrusting of this region over the South Caspian basin from the west.

3. Deep seismic data

Here are presented some of the first deep seismic reflection profiles-ABSHERON 1 and 2-recorded to 20 s (~50 km) in the South Caspian Sea (Fig. 1). Each approximately 70 km in length, the ABSHERON profiles were recorded in the deep water (200–700 m) of the South Caspian Sea, offshore Azerbaijan, at the Absheron Ridge (Fig. 1). These profiles were acquired with industry-like marine acquisition parameters (Table 1), using a Syntrak-480 telemetric digital recording system with 204-channels and linear arrays of 16 hydrophones deployed every 25 m. The maximum offset was 5300 m. A 0.052 m^3 airgun at 1900 psi was deployed every 50 m in order to provide the acoustic energy.

Processing of the deep seismic ABSHERON data was focused on enhancing the low-energy deep reflections and removing the abundant multiple energy commonly observed in marine seismic reflection data. The processing sequence included trace editing, spherical divergence correction, trace-to-trace amplitude balance, time-variant amplitude scaling, time-variant frequency filtering, velocity analysis, normal-moveout (NMO), common mid-point stacking (~50-fold), and finite-difference post-stack time migration (Table 2). In order to preserve the amplitude and frequency content of the data at the various depth levels, time-dependent processing including amplitude scaling and

Table 1
Acquisition parameters of the ABSHERON profiles

Airgun source	0.052 m^3 at 1900 psi
Shotpoint interval	50 m
Recording length	20.0 s
Sample rate	4 ms
Receiver array	16 Hydrophones, in linear array
Group spacing	25 m
No. of groups	204
Streamer length	5100 m
Minimum offset	250 m
Maximum offset	5350 m
Spread configuration	End-on

Table 2
Processing sequence of the ABSHERON profiles

Processing	Parameters
Pre-stack	
Resample data	8 ms
Geometry	
Spherical divergence correction	w/stacking velocities
Trace equalization	20 s
Time variant amplitude scaling	0–5, 5–10, 10–15, 15–20 s, with 1.5 s window
Predictive deconvolution	140 ms operator length
Time variant bandpass filter	8–12–55–62 Hz @ 0–5 s 6–10–50–57 Hz @ 5–10 s 4–8–45–52 Hz @ 10–15 s 4–8–40–47 Hz @ 15–20 s
F-X decon (Wiener Levinson)	Time window 300 ms
t-p filter	Dip of 6 traces/s
NMO	w/stacking velocities
Radon filer	
Top mute	
CDP median stack	
Post-stack	
Time variant amplitude scaling	0–5, 5–10, 10–15, 15–20 s
Bandpass filter	4–8–50–55 Hz
F-X decon (Wiener Levinson	Time window 300 ms
t-p filter	Dip of 6 traces/s
Enhancement 2D spatial filter	Mix of 3 traces
FD time migration	w/stacking and refraction velocities refraction
Depth conversion	w/stacking and refraction velocities refraction

frequency filtering was performed instead of the application of the standard automatic gain control (AGC) and bandpass filters. Predictive deconvolution (Taner, O'Doherty, & Baysal, 1991), tau-p (intercept time-ray parameter) dip filter (Stoffa, Buhl, Diebold, & Wenzel, 1981), and Radon filter (Hampson, 1986) were used for the suppression of the redundant reflected energy. The tau-p transform was also used to enhance the coherent seismic energy. Through this process, the input offset-time seismic traces were transformed into a selected range of dip (slant-stacked) traces that were weighted by the semblance along the respective dips. This is the tau-p domain. These dip traces were transformed back into the offset-time domain (Stoffa et al., 1981). The Radon filter was used in the common depth point (CDP) domain for the suppression of unwanted multiple energy (Hampson, 1986). Through this technique, the multiples that were identified through their residual move-outs after the application of NMO, were modeled and subsequently subtracted from the input traces.

The stacked seismic data in the CDP domain were migrated using the time domain explicit finite-difference algorithm (Soubaras, 1992). This algorithm best handles vertical and lateral variable interval velocity fields in time as well as moderate dips of the reflectors as these features are noticeable in the unstacked data. The migration and conversion to depth were based on a velocity function derived from (1) velocity analysis of the top 10.0 s based on NMO correction, and (2) velocities provided by previous DSS and receiver function data for the time interval between 10.0 and 20.0 s [@7.0 km/s average velocity (Baranova et al., 1991; Galperin et al., 1962; Gegelyantz et al., 1958; Mangino & Priestley, 1998)]. However, in order to facilitate an easy comparison of the unmigrated and migrated data, both the unmigrated and migrated sections are provided for each of the two profiles and displayed at the same scale with no vertical exaggeration (Figs. 2 and 3).

Stacked (Figs. 2a and 3a), migrated, and depth converted (Figs. 2b and 3b) seismic sections of the near-vertical incidence shot gathers of the ABSHERON profiles suggest that the South Caspian crust in the vicinity of the Absheron Ridge is highly reflective despite the variability in the lateral continuity of the reflectors, especially at large depths. Although recorded with petroleum industry parameters (Table 1), the ABSHERON profiles provide seismic reflections at all crustal levels, down to ~16.0–17.0 s. However, there were significant systematic lateral variations in the amount of energy penetrating the crust. A detailed analysis of the reflection amplitudes along the ABSHERON lines was performed through amplitude decay analysis (Figs. 2a and 3a) that were computed from the edited but unprocessed CMP (common mid-point) gathers in order to determine the limits of seismic signal penetration on the deep seismic reflection data (e.g. Barnes, 1994). These curves were computed at representative CMP locations along the ABSHERON lines (A–E in Fig. 2a and F–I in Fig. 3a), where a dramatic change in the reflective character is noticeable at the crustal levels below ~10.0 s. Note that the maximum amplitude (in db) is recorded at the surface (Figs 2a and 3a). The basic assumption is that for a given CMP, the decaying amplitude is a measure of the signal penetration power at that depth (e.g. Barnes, 1994). Hence, a decaying amplitude curve suggests sufficient seismic energy whereas no decay, or a flat curve, implies a lack of signal penetration. As seen along the ABSHERON 2 profile, the amplitude decay curves A and C suggest decay down to ~16 s whereas B, D, and E stop decaying at much shallower levels (~10–11 s). Similarly, F and I along the ABSHERON 1 profile decay down to at least 16 s, while G and H are fairly flat below ~11 s.

The presence of large, high-amplitude structures in the upper part of the sedimentary section may cause the acoustic phenomenon called focusing (Sheriff & Geldart, 1995) that appears to be responsible for the reduction in reflectivity below the convex structures (anticlines), and the increase in reflectivity beneath the concave structures (synclines). Since these profiles were collected with industry acquisition parameters, inconsistent signal penetration along the profiles may be a result of both geometric spreading and focusing by large-scale shallow structures and insufficient source effort (0.052 m^3 airgun) for imaging at large depths.

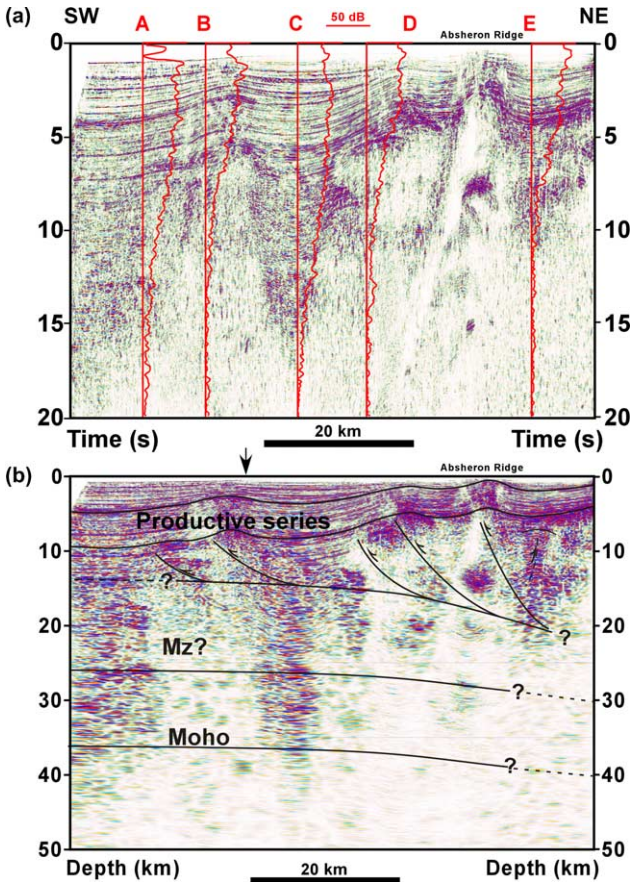

Fig. 2. Crustal-scale seismic reflection image of the South Caspian basin from the ABSHERON 2 profile. (a) Unmigrated CDP stack of the ABSHERON 2 profile, oriented NE–SW across the Absheron Ridge, shows several key features, including (1) large-scale folds which deform the shallow sedimentary section, (2) prominent reflection at ~13 s on southern end of profile, (3) change in reflection character (amplitude and frequency) below ~13 s, and (4) decrease in reflectivity below ~16 s. Amplitude decay curves calculated from CDP gathers are displayed in red, and show a strong correlation with the seismic reflection image suggesting that non-reflective areas above 16 s are a result of poor signal penetration. (b) Finite-difference migrated and depth-converted seismic image with overlying interpretation. While features cannot be traced continuously across the section due to imaging problems, the reflection character can be correlated laterally. Bright reflection at ~26–28 km depth (12.8–13.0 s), with an apparent gentle northward dip, is interpreted as the basement/cover contact. Downward termination of reflectivity at ~34–38 km (15.5–16.0 s) is thought to represent the Moho, despite the absence of a clearly reflective horizon. The seismic image in the northern part of the line is distorted by the presence of a mud volcano in the vicinity of the Absheron Ridge (Diaconescu, Kieckhefer, & Knapp, 2001). The high amplitude event at ~7.0–8.0 s (12–15.5 km) beneath the Absheron Ridge represents diffractive energy from the water column, with $V_P = 1.1$ km/s. Question marks are uncertainties in the interpretation. Arrow marks intersection with ABSHERON 1 line. No vertical exaggeration has been applied.

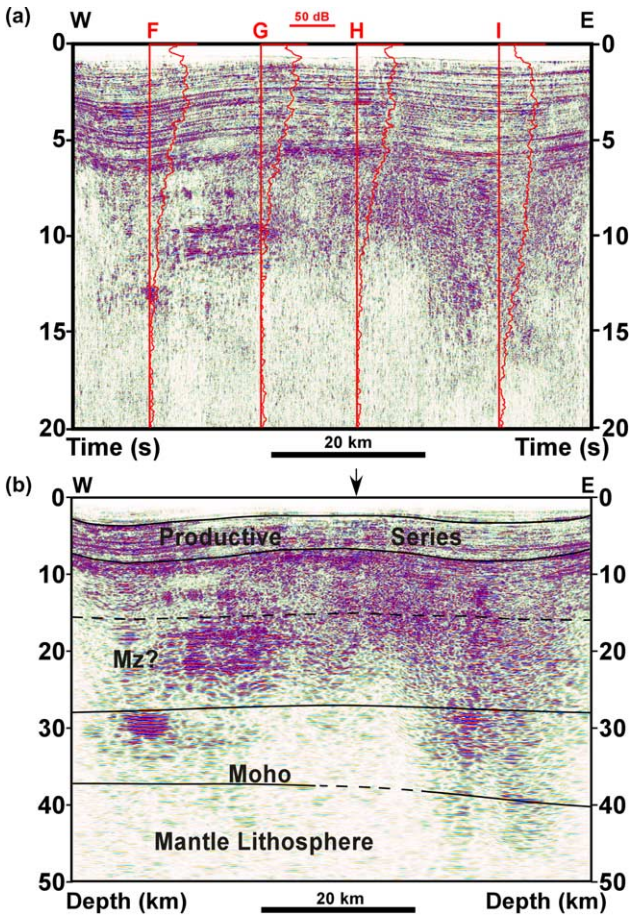

Fig. 3. Crustal-scale seismic reflection image of the South Caspian basin from the ABSHERON 1 profile. (a) Unmigrated CDP stack of the ABSHERON 1 profile oriented E–W sub-parallel to the Absheron Ridge. Amplitude decay curves shown in red overlay the seismic section, and show a relatively poor signal penetration to Moho traveltimes along most of this profile. (b) Finite-difference migrated and depth-converted seismic image with overlying interpretation. Identification of major structural/lithologic boundaries was based primarily on tie with ABSHERON 2 profile, and changes in character of reflective packages with depth. Distinct reflections, interpreted as the Moho, can be identified at 38–40 km depth, consistent with known velocity models and the ABSHERON 2 profile. No vertical exaggeration has been applied.

Hence, the lateral variations of the amplitude decay curves with depth may suggests that the highly variable lateral changes in the reflective character along the ABSHERON lines is more likely a result of poor signal penetration beneath the anticlines rather than an effect of lithologic or structural changes at depth. The seismic image in the northern part of the ABSHERON 2 line is distorted by the presence of a mud volcano beneath the Absheron Ridge.

The ABSHERON 2 profile has a critical position within the South Caspian basin since it crosses the Absheron Ridge which represents (1) the site of ~4 billion barrels (BBOE) of proven oil reserves (Devlin et al., 1999), (2) a sharp change from transpressional deformation in the east (Turkmenistan lowlands) to compression in the west (Neogene collision in the Caucasus Mountains), and (3) the locus of deep crustal and mantle earthquakes (e.g. Jackson et al., 2002; Priestley et al., 1994). Some of the most noticeable features displayed by the ABSHERON 2 profile and shown in Fig. 2a and b are: (1) a series of high-amplitude folds developed within the thick Tertiary–Quaternary portion of the section down to ~7.0 s, (2) a strongly reflective horizon at ~12.8–13.0 s on the southern

part of the profile, (3) an underlying layered reflective interval down to ~15.5–16.0 s with discernibly lower frequency reflections, and (4) a noticeable decrease in reflectivity below ~16 s (Fig. 2a and b). Note the good correlation between the abundant/lack of deep (10–16 s) reflections along the profile with the amplitude decay curves, suggesting that were present, the deep crustal reflectors occur within the limits of signal penetration, and are likely to be real interfaces rather than artifacts generated during the data processing (Fig. 2a).

Below the deformed sedimentary strata, the south-western end of the ABSHERON 2 profile is dominated by a highly reflective subhorizontal reflector approximately 10 km long at ~13 s. Due to the poor seismic imaging at this depth, this reflector disappears for ~15 km but can be traced again toward the center of the profile. This reflector is not imaged on the north-eastern half of the line since the seismic image is distorted by the presence of a mud volcano. On the migrated depth section (Fig. 2b), this strong reflector is observed at ~26 km depth, and appears to have a slight northward dip toward the center of the line based on which it was traced toward the Absheron Ridge down to depths as large as ~28–30 km.

Line ABSHERON 1 is almost perpendicular to line ABSHERON 2 (Fig. 1), and the identification of the major structural and lithologic boundaries was based primarily on the tie with the ABSHERON 2 profile as well as the changes in the character of the reflective packages with depth (Fig. 3a and b). The shallow portion of the section is characterized by abundant coherent reflectivity to 10–11 s (25–27 km), which dies out in the underlying layer. However, distinct reflective packages can be observed at 12–15 s (28–40 km) in the western and eastern parts of the profile. As noticed in the ABSHERON 2 profile, there is a direct correlation between the lack of seismic reflectivity at large depths and the lack of decay on the amplitude curves (Fig. 3a). This suggests a relatively poor signal penetration to large depths along the central part of this profile.

4. Discussion

The ABSHERON seismic data presented here provide one of the first whole crustal-scale seismic reflection images of the South Caspian basin in the vicinity of the Absheron Ridge. Due to its strong reflective character as well as a noticeable change in the reflective pattern across this boundary from higher to lower frequencies, the bright reflector at ~26–28 km depth (12.8–13.0 s) is interpreted as the basement/cover contact (Fig. 2a and ba and b). The overlying seismic section shows no obvious change in the amplitude and frequency content of reflections, whilst below this horizon the reflectivity is noticeably of lower frequency and higher amplitude. In addition, previous velocity models from both DSS and teleseismic studies in the South Caspian area (Baranova et al., 1991; Mangino & Priestley, 1998; Zonenshain & Le Pichon, 1986) suggested a minimum sedimentary thickness of 20 km, precluding a shallower basement/cover contact. This reflector is the highest amplitude and the most continuous seen on the ABSHERON 2 line below 14 km. Although laterally discontinuous, this bright reflector can be traced toward the Absheron Ridge, exhibiting a gentle northward dip. If correct, these observations imply that the sedimentary fill of the South Caspian basin is ~26–28 km in thickness, and thickens to ~30 km in the vicinity of the Absheron Ridge, making it one of, if not, the thickest sedimentary basin.

The interpretation of a 26–28 km thick sedimentary section in the South Caspian basin is in good agreement with results from previous DSS data (Baranova et al., 1991; Galperin et al., 1962; Gegelyantz et al., 1958; Zonenshain et al., 1990; Zonenshain & Le Pichon, 1986) as well as teleseismic receiver functions (Jackson et al., 2002) that suggested 20 + km thick sediments accumulated in the South Caspian basin. Reprocessing of the earlier DSS data by Baranova et al. (1991), suggested that the basement/cover contact occurs at ~27–28 km depth beneath the South Caspian basin in the vicinity of the Absheron Ridge based on a sharp velocity contrast from 4.8 to 6.6 km/s. Note that the relatively reduced velocities are also confirmed by the presence of numerous mud volcanoes in the study area, that suggest a highly deforming petroleum bearing basin characterized by high sedimentation rates in the Cenozoic, significant thicknesses of the sedimentary cover (>10 km), and abnormally high pore pressures.

The upper ~14–20 km (8–10 s; Fig. 2a and b) of the ABSHERON 2 section are dominated by a sequence of large, open folds that show (1) a subtle but noticeable asymmetry, with shallower northern limbs and steeper southern limbs, and (2) progressively more open and structurally deeper fold hinges from N to S. Stratigraphy within these folds shows a marked discordance with both subhorizontal reflections below ~14 km depth, and a gently N-dipping, high-amplitude reflector observed on the migrated seismic section (approximately in the middle of the section). Based on these observations, we interpret these fold structures to be S-vergent fault-propagation folds that root into a detachment that appears to deepen northward from ~14 to 20 km (8–10 s; Fig. 2a and b). Although this interpretation is admittedly not unique, the observed fold geometries do not appear to be consistent with the buckle-style folding observed further southward in the basin (Devlin et al., 1999). Such structural geometries are not only commonplace in most deformed sedimentary sections, but are dictated by the pronounced anisotropies resulting from the sedimentary layering. Based on this interpretation, the position of the detachment can be extrapolated down to ~20 km toward the north-eastern side of the profile.

The seismic section below ~28 km (~13.0 s; Figs. 2a and b) is interpreted as crystalline basement. Downward termination of reflectivity is thought to represent the Moho, despite the absence of a clearly reflective horizon, making

for a composite crustal thickness in this portion of the basin of ~36–40 km (15.5–16.0 s). Based on the ABSHERON seismic profiles, we suggest that the South Caspian crust is ~10 km thick in our study area. Both the apparent lack of local structural relief on the basement reflector and the high seismic velocities ($V_p \approx 6.8$ km/s) obtained from earlier studies suggest that this crust is not thinned continental material. This interpretation agrees with the earlier DSS regional studies of the Caspian Sea region (Baranova et al., 1991; Galperin et al., 1962; Gegelyantz et al., 1958; Mangino & Priestley, 1998; Zonenshain et al., 1990; Zonenshain & Le Pichon, 1986), which suggested a total crustal thickness of ~30–40 km beneath the Absheron Ridge. The apparent ~10 km thickness of the crystalline crust is certainly much thinner than a common continental crust (Kerr, 1984), and we suggest that it has an oceanic affinity in this part of the basin (Mangino & Priestley, 1998; White, McKenzie, & O'Nions, 1992).

Some of the previous studies have characterized the oceanic lower crust as reflective and underlain by a sharp Moho (Cernobori, Hirn, McBride, Nicolich, & Romanelli, 1996; McBride, White, Henstock, & Hobbs, 1994). The ABSHERON data suggest that the crust flooring the South Caspian basin is reflective and the Moho does not appear as a sharp boundary, but rather as a downward termination of abundant reflectivity in the southern part of the ABSHERON 2 line (Fig. 2a and b). The distinctive reflective packages at 12–15 s (28–40 km) in the western and eastern parts of the ABSHERON 1 profile are interpreted as crystalline crust. The Moho is identified here at 38–40 km depth from the downward termination of reflectivity, consistent with known velocity models and the results from the ABSHERON 2 profile. Slight deepening of the Moho from west to east (Fig. 3b) may suggest a thickening of the crust toward the Kopeh-Dagh fold belt inferred to be floored by continental crust (Berberian, 1983; Mangino & Priestley, 1998; Nadirov et al., 1997).

The interpretation presented here for the crustal architecture of the South Caspian basin in the vicinity of the Absheron Ridge is also well-constrained by earlier gravity studies. A free-air gravity anomaly of −130–150 mgal has been observed in the northwestern part of the South Caspian basin along the ABSHERON 2 profile, and is consistent with a thick (26–28 km) accumulation of sediments and a relatively thin oceanic crust (Granath & Baganz, 1997; Sandwell & Smith, 1997). Recent gravity modeling of the free air gravity data performed on an alignment approximately coincident with the position of the ABSHERON 2 profile (Granath, Soofi, Baganz, & Baghirov, 2000; Kadirov, 2000), suggests that the South Caspian Sea is floored by an ~10 km thick, high density crust (~2.9 g/cm^3), consistent with oceanic affinity. The negative gravity anomaly across the Absheron Ridge has been interpreted as underthrusting of the South Caspian lithosphere beneath the Central Caspian lithosphere at this boundary.

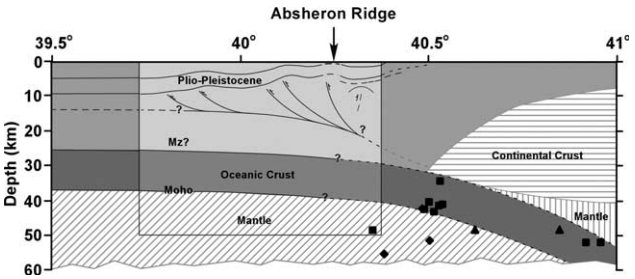

Fig. 4. Subduction model of the South Caspian lithosphere beneath the Eurasian continent at the Absheron Ridge. The rectangle delineates the region coincident with line ABSHERON 2 (darker gray shades). The position of the basement/cover contact, the basal detachment of the major structures, and the Moho are displayed. The Cenozoic/Mesozoic sedimentary section attains a stratigraphic thickness of 26 km on the southern end of the profile, and is structurally thickened to 30 + km on the northern end of the profile. Diamonds represent published earthquake foci (Priestley et al., 1994), squares are earthquake foci from the International Seismological Center (ISC, 1964–1994), and triangles are earthquake foci from the Centroid-Moment Tensor catalog (CMT, 1977–1996). All the earthquakes displayed have magnitudes greater than 5.0. The earthquakes occur north of the Absheron Ridge, and most of them cluster within the prolongation of our interpreted mantle lithosphere. Information outside the ABSHERON 2 profile is compiled from existing DSS and teleseismic receiver function data (Mangino & Priestley, 1998; Zonenshain et al., 1990; Zonenshain & Le Pichon, 1986). Horizontal units represent latitude in degrees east. Question marks represent uncertainties in the interpretation. Arrow marks intersection with ABSHERON 2 line. No vertical exaggeration.

The gentle northward deepening of the crust on the ABSHERON 2 profile is interpreted as evidence for northward subduction of the South Caspian lithosphere beneath the Central Caspian lithosphere across the Absheron Ridge (Fig. 4). This interpretation is supported by active subcrustal (down to 80 km) seismicity that occurs north of the Absheron Ridge (Fig. 1; Jackson et al., 2002; Priestley et al., 1994). Note that most of the earthquake hypocenters occur within the interpreted South Caspian subducting crust, only with a few events in the mantle lithosphere (Fig. 4). There are a relatively limited number of mechanisms we know of to generate seismicity in the continental mantle lithosphere. Subduction of oceanic plates is well-established as a source for mantle seismicity, and delamination of thickened lithospheric mantle has been proposed as a mechanism in other regions (Seber et al., 1996). Note that thrusts which core the shallow folds on line ABSHERON 2 (Figs. 2b and 4) are consistent with northward subduction of South Caspian Sea lithosphere, but these faults do not cut the overlying productive series. Teleseismic receiver function and earthquake studies (Jackson et al., 2002; Mangino & Priestley, 1998) suggested the South Caspian basin is floored by oceanic crust that likely subducts beneath continental crust at the Absheron Ridge.

Previous studies of focal mechanism for earthquakes at the Absheron Ridge (Jackson et al., 2002; Priestley et al., 1994) suggested the occurrence of a combination of shallower normal-faulting events parallel to the ridge (30–50 km), and deeper (50–75 km) thrust fault events

further to the north-east (Figs. 1 and 4). The lack of upper crustal seismicity, based on these studies, was interpreted as an aseismic shortening of the South Caspian sedimentary cover at the Absheron Ridge. The deeper thrust events were interpreted as a result of shortening, probably caused by the onset of subduction of the South Caspian lithosphere beneath the Eurasian continental crust of the Central Caspian basin at the Absheron Ridge (Jackson et al., 2002).

While the ABSHERON data provide new constraints on the crustal structure of the South Caspian basin, the mechanism for accelerated subsidence in the Plio-Pleistocene remains unclear. Incipient subduction beneath the Absheron Ridge might be invoked (Allen et al., 2002), but such a mechanism would presumably result in a thickened stratigraphic sequence along the entire ridge. The ABSHERON data do not constrain such a model, and existing isopach data do not appear to be consistent with such an interpretation (Zonenshain & Le Pichon, 1986).

5. Conclusions

Deep (20 s; 50 km) seismic reflection (ABSHERON) data from the South Caspian Sea region in the vicinity of the Absheron Ridge suggest that the South Caspian basin is covered by a very thick (26–28 + km) sedimentary cover, making it one of, if not, the thickest basin in the world. The thick (~14–18 km) Cenozoic sedimentary section of the South Caspian basin as seen on the ABSHERON profiles seems to be dominated by a S-vergent fold and thrust system that appears to be rooted into an intra-sedimentary detachment dipping northward at a depth of ~14–20 km. Although slightly thicker than observed in other ocean basins, the apparent ~10 km thick crystalline crust is consistent with an oceanic affinity for this part of the basin. Active seismicity and gentle deepening of the crust from south to north are interpreted as evidence for northward subduction of the South Caspian oceanic lithosphere beneath the southern margin of Eurasia.

Acknowledgements

Many thanks are due to Chevron Overseas Petroleum Inc. (USA), SOCAR (Azerbaijan), and Total (France) for providing the seismic data. John McBride, Larry Brown and Eugenio Asencio provided useful comments during the progress of this work. Acknowledgment is made to the donors of The Petroleum Research Fund, administered by the ACS, for support of this research.

References

Adamia, S. A., Buadze, V. I., & Shavishvili, I. D. (1977). The Great Caucasus in the Phanerozoic; A geodynamic model. In S. Jankovic (Ed.), *Metallogeny and plate tectonics in the northeastern Mediterranean* (pp. 215–229).

Allen, B. M., Vincent, S. J., Ismail-zadeh, A., Simmons, M., & Anderson, L. (2002). Onset of subduction as the cause of rapid Pliocene–Quaternary subsidence in the South Caspian basin. *Geology*, *30*(9), 775–778.

Amursski, G. I., Tiunov, K. V., Khrikov, B. A., & Shlezinger, A. E. (1968). Structure and tectonic position of the Great Balkhan. *Akademii Nauk SSR*, 53.

Avdeev, D. B., Dubrovski, V. G., Fainberg, E. B., Pankratov, O. V., & Zinger, B. S. (1984). Deep electromagnetic sounding in Turkmenia. *Geophysical Journal International*, *118*, 467–484.

Bagirov, E., & Lerche, I. (1999). Rising mud diapirs and their thermal anomalies. *Computer Applications in the Earth Sciences*, 203–218.

Baranova, E. P., Kosminskaya, I. P., & Pavlenkova, N. I. (1991). A reinterpretation of South Caspian DSS Data. *Geophysical Journal*, *10*(5), 666–677.

Barnes, A. E. (1994). Moho reflectivity and seismic signal penetration. *Tectonophysics*, *232*(1–4), 299–307.

Berberian, M. (1983). The Southern Caspian: A compressional depression floored by trapped, modified oceanic crust. *Canadian Journal of Earth Sciences*, *20*, 163–183.

Brunet, M.-F., Korotaev, M. V., Ershov, A. V., & Nikishin, A. M. (2003). The South Caspian Basin: A review of its evolution from subsidence modeling. *Sedimentary Geology*, *156*, 119–148.

Brunet, M.-F., Volozh, Y. A., Antipov, M. P., & Lobkovsky, L. I. (1999). The geodynamic evolution of the Precaspian Basin (Kazakhstan) along a north-south section. *Tectonophysics*, *313*, 10–85.

Cernobori, L., Hirn, A., McBride, J. H., Nicolich, R. P. L., & Romanelli, M. (1996). Crustal image of the Ionian Basin and its Calabrian margins. *Tectonophysics*, *264*, 175–189.

Curray, J. R., Emmel, F. J., Moore, D. G., & Raitt, R. W. (1982). Structure, tectonics, and geological history of the northeastern Indian Ocean. In A. E. M. Nairn, M. Churkin, Jr., & F. G. Stehli (Eds.), *The ocean basins and margins* (pp. 399–450). New York: Plenum Press.

Devlin, W. J., Cogswell, J. M., Gaskins, G. M., Isaksen, G. H., Pitcher, D. M., Puls, D. P., Stanley, K. O., & Wall, G. R. T. (1999). South Caspian Basin; Young, cool, and full of promise. *GSA Today*, *9*, 1–9.

Diaconescu, C. C., Kieckhefer, R. M., & Knapp, J. H. (2001). Geophysical evidence for and thermobaric modeling of gas hydrates in the deep water of the South Caspian Sea, Azerbaijan. *Marine and Petroleum Geology*, *18*(2), 209–221.

Galperin, Y., Kosminskaya, I., & Kraksina, P. (1962). *Main characteristics of deep waves recorded during deep seismic sounding in central part of Caspian Sea. In: Deep seismic sounding of the Earth's crust in the USSR*, Moscow: Acad. Sci. USSR, in Russian.

Gegelyantz, A. A., Galperin, E. N., Kosminskaya, I. P., & Krafshina, R. M. (1958). Structure of the Earth's crust in the central part of Caspian Sea from deep seismic sounding data. *Doklady Akademii Nauk SSSR*, *123*, 520–522. in Russian.

Granath, J. W., & Baganz, O. W. (1997). Late Neogene tectonics of the South Caspian Basin, Azerbaijan. *AAPG Bulletin*, *81*(8), 1378–1379.

Granath, J. W., Soofi, K. A., Baganz, O. W., & Baghirov, E. (2000). Gravity modeling and its implications to the tectonics of the South Caspian basin. *AAPG Inaugural Regional International Conference, Extended Abstracts*, 46–49.

Grotzinger, J. P., & Ingersoll, R. V. (1992). Proterozoic sedimentary basins. In J. W. Schopf, & C. Klein (Eds.), *The Proterozoic biosphere; A multidisciplinary study* (pp. 47–50). Cambridge, UK: Cambridge University Press.

Hampson, D. (1986). Inverse velocity stacking for multiple elimination. *Journal of the Canadian Society of Exploration Geophysicists*, *22*, 44–55.

Jackson, J. (1992). Partitioning of strike–slip and convergent motion between Eurasia and Arabia in eastern Turkey and the Caucasus. *Journal of Geophysical Research, B, Solid Earth and Planets*, *97*, 12471–12479.

Jackson, J., Priestley, K., Allen, M., & Berberian, M. (2002). Active tectonics of the South Caspian Basin. *Geophysical Journal International*, *148*, 214–245.

Jarchow, C. M., & Thompson, G. A. (1989). The nature of the Mohorovicic discontinuity. *Annual Review of Earth and Planetary Sciences*, *17*, 475–506.

Kadirov, F. A. (2000). Application of the Hartley transform for interpretation of gravity anomalies in the Shamakhy-Gobustan and Absheron oil- and gas-bearing regions, Azerbaijan. *Journal of Applied Geophysics*, *45*(1), 49–61.

Kerr, R. A. (1984). Probing the deep continental crust. *Science*, *225*, 492–494.

Mangino, S., & Priestley, K. (1998). The crustal structure of the southern Caspian region. *Geophysical Journal International*, *133*, 630–648.

McBride, J. H., White, R. S., Henstock, T. J., & Hobbs, R. W. (1994). Complex structure along a Mesozoic sea-floor spreading ridge; BIRPS deep seismic reflection, Cape Verde abyssal plain. *Geophysical Journal International*, *119*, 453–478.

McKenzie, D. (1978). Some remarks on the development of sedimentary basins. *Earth and Planetary Science Letters*, *40*, 25–32.

McKenzie, D., Nisbet, E., & Sclater, J. G. (1980). Sedimentary basin development in the Archaean. *Earth and Planetary Science Letters*, *48*, 35–41.

Nadirov, R. S., Bagirov, E. B., Tagiyev, M. F., & Lerche, I. (1997). Flexural plate subsidence, sedimentation rates, and structural development of the super-deep South Caspian Basin. *Marine and Petroleum Geology*, *14*(4), 383–400.

Priestley, K., Baker, C., & Jackson, J. (1994). Implications of earthquake focal mechanism data for the active tectonics of the South Caspian basin and surrounding regions. *Geophysical Journal International*, *118*, 111–141.

Sandwell, D. T., & Smith, W. H. F. (1997). Marine gravity anomaly from Geosat and ERS 1 satellite altimetry. *Journal of Geophysical Research, B, Solid Earth and Planets*, *102*(5), 10039–10054.

Seber, D., Barazangi, M., Ibenbrahim, A., and Demnati, A. (1996). Geophysical evidence for lithospheric delamination beneath the Alboran Sea and Rif-Betic mountains. *Nature*, *379*, 785–790.

Sheriff, R. E., & Geldart, L. P. (1995). *Exploration seismology*. Cambridge, UK: Cambridge University Press, pp. 592.

Shikalibeily, E. S., & Grigoriants, B. V. (1980). Principal features of the crustal structure of the South-Caspian Basin and the conditions of its formation. *Tectonophysics*, *69*(1/2), 113–121.

Shlezinger, A. Y., & Yanshin, A. L. (1981). Tectonic non-uniformity of the world ocean floor. *Sovetskaya Geologiya*, *1981*(7), 41–50.

Soubaras, R. (1992). Explicit 3-D migration using equiripple polynomial expansion and Laplacian synthesis. *SEG Annual Meeting Expanded Technical Program Abstracts with Biographies*, *62*, 905–908.

Stoffa, P. L., Buhl, P., Diebold, J. B., & Wenzel, F. (1981). Direct mapping of seismic data to the domain of intercept time and ray parameter; A plane-wave decomposition. *Geophysics*, *46*, 255–267.

Taner, M. T., O'Doherty, R. F., & Baysal, E. (1991). Multiple suppression by multi-channel predictive deconvolution. *Technical Programme and Abstracts of Papers—European Association of Exploration Geophysicists*, *53*, 22–23.

Watts, T. (1992). The formation of sedimentary basins. In G. C. Brown, C. J. Hawkesworth, & R. C. L. Wilson (Eds.), *Understanding the Earth* (pp. 301–324). Cambridge, United Kingdom: Cambridge University Press.

White, R. S., McKenzie, D., & O'Nions, R. K. (1992). Oceanic crustal thickness from seismic measurements and rare earth element inversions. *Journal of Geophysical Research B, Solid Earth and Planets*, *97*, 19683–19715.

Zonenshain, L. P., Kuzmin, M. I., & Natapov, L. M. (1990). Geology of the USSR: A plate tectonic synthesis. In B. M. Page (Ed.), *Geology of the USSR: A plate tectonic synthesis* (*Vol. 21*) (pp. 169–198). *Geodynamic Series*, Washington, DC: American Geophysical Union.

Zonenshain, L. P., & Le Pichon, X. (1986). Deep basins on the Black Sea and Caspian Sea as remnants of Mesozoic back-arc basins. *Tectonophysics*, *123*, 181–211.